J Clust Sci (2017) 28:2635–2643
DOI 10.1007/s10876-017-1245-6

ORIGINAL PAPER

Synthesis and Characterization of Spindle-Like TiO_2 Nanostructures and Photocatalytic Activity on Methyl Orange and Methyl Blue Dyes Under Sunlight Radiation

S. Arunkumar[1] · M. Alagiri[1]

Received: 9 April 2017 / Published online: 8 June 2017

Abstract Spindle-like TiO_2 nanostructures was prepared by a simple one pot solvothermal method followed by calcination at 400 °C for 3 h. The sample was characterized using various techniques such as X-ray diffractometer, transmission electron microscopy, Fourier transform infrared spectroscopy and UV–Vis absorption spectroscopy. The crystal structure of TiO_2 nanostructure was measured by X-ray diffractometer. According to the XRD result, the peaks in the sample can be indexed to anatase phase of TiO_2. The morphological characterization of TiO_2 sample was examined by transmission electron microscopy. The synthesized sample consisted of spindle-like shape with size in the range of 50–70 nm. The band gap value of Spindle-like TiO_2 nanostructures is 2.92 eV, which is lower than that of bulk TiO_2 of 3.2 eV. The FTIR bands observed at 493, 443 and 428 cm^{-1} confirms the presence of TiO_2. The Spindle-like TiO_2 nanostructures showed photodegradation ability for methyl orange and methyl blue dye. The reuse evaluation of the Spindle-like TiO_2 nanostructures showed that their photocatalytic activity had good durability.

Keywords Spindle-like TiO_2 nanostructures · Optical properties · X-ray diffraction · Methyl orange · Methyl blue

✉ M. Alagiri
alagiri.m@ktr.srmuniv.ac.in

[1] Center for Material Science and Nano Devices, Department of Physics and Nanotechnology, SRM University, Kattankulathur, Kancheepuram (D.T), Tamil Nadu 603203, India

Introduction

Over the past several years, the widespread use of large volume of coloured dyes has resulted in their unwanted accumulation in the environment. Dyes are soluble in water and have been identified in groundwater. Hence, water pollution has become a global issue, resulting in a serious adverse effect on public life and the environment [1, 2]. To overcome this problem, considerable efforts have been made such as photocatalytic degradation [3–5], adsorption [6], chemical oxidation [7], flotation [8], solvent extraction [9] and filtration [10]. Among these, photocatalytic degradation of organic pollutants has received considerable attention owing to its high efficiency, low cost, simplicity and this process does not require external power source since the absorption of solar energy is enough to degrade the organic pollutants.

Up to date, various photocatalysts have been introduced for the degradation of organic dyes, including TiO_2 [11], ZnO [12], Cu_2O [13], CdS [14] etc. Among the above photocatalysts, Titanium dioxide (TiO_2) has attracted considerable attention in pollution control, sensors, Li batteries, energy storage, photovoltaics and due to its unique photoelectric properties, nontoxicity, high chemical stability and low cost. TiO_2 can exist in three different crystallographic phases namely brookite (orthorhombic), rutile (tetragonal) and anatase (tetragonal). According to the literature, anatase phase is photocatalytically more active than brookite or rutile phases due to the low recombination rate between photogenerated electrons and holes on the surface of TiO_2 [15]. The performance of Photocatalytic activity on TiO_2 relies on the morphology. Recently, TiO_2 spindle-shaped nanoporous anatase material has attracted great attention owing to their following features. Firstly, spindle-like TiO_2 nanoporous materials with large surface areas have proved to be excellent photocatalysis. Secondly, nanoporous materials can enhance the adsorption. Thirdly, they can be easily recycled from a solution by sedimentation [16]. Many methods have been developed to synthesis TiO_2 nanostructures including sol-gel template method [17], hydrothermal method [18], chemical vapor deposition [19], electrochemical deposition [20], Solvothermal method [21], microwave [22] and electrospinning [23]. To the best of our knowledge the degradation of methyl orange and methyl blue dyes under sunlight radiation using spindle-like TiO_2 nanostructure have not been yet reported. In this study, we report the preparation of TiO_2 photocatalyst by solvothermal method and its characterization. Also, the photocatalytic activity of the spindle-like TiO_2 nanostructures were analyzed by degradation of methyl orange (MO) and methyl blue (MB).

Experiments

Preparation of Spindle-Like TiO_2 Nanostructures

The method used for the synthesis of spindle-like TiO_2 nanostructures as follows: In typical synthesis, 1.5 ml of titanium n-butoxide (TBT) was was added to 80 ml of

acetic acid with 2 h of stirring and the pH of the solution was adjusted by adding 1.0 M NaOH. The solution was stirred continuously for 3 h. Then, the mixture solution was transferred into a Teflon-lined stainless steel autoclave with a capacity of 100 ml sealed and maintained at 190 °C for 24 h. The autoclave was then allowed to cool from 190 °C to room temperature. The prepared sample was centrifuged then rinsed with distilled water and ethanol several times to remove any impurities that remained in the sample and finally dried in an oven at 80 °C. To obtain pure anatase TiO_2 phase, the as-synthesized powder sample was calcined at 400 °C for 3 h.

Characterizations of Spindle-Like TiO_2 Nanostructures

The X-ray powder diffraction pattern of the sample was carried out with a PANalytical (X'pert PRO) X-ray diffractrometer using $CuK\alpha_1$ radiation ($\lambda = 1.5406$ Å). An FTIR study on the prepared sample was carried out from 400 to 4000 cm^{-1} with a Perkin Elmer spectrometer. TEM and HRTEM images were recorded on a JEOL 3010 instrument. The optical absorption spectrum of the sample and progress of the photocatalytic reaction were measured by UV–Vis absorption studies on a Specord 200 plus, Analytikjena.

Photocatalytic Activity of Spindle-Like TiO_2 Nanostructures

Photocatalytic activity of spindle-like TiO_2 nanostructure was evaluated by studying photodegradation of MO and MB dye solutions under sunlight radiation. The experiment was performed between 11.00 a.m. and 1.30 p.m. under direct sunlight. Typically, 50 mg of as synthesized TiO_2 photocatalyst was dispersed in 50 ml of 0.03 mM aqueous MO or MB dye solution (10 mgl^{-1}). Before sunlight irradiation, the solution was stirred at room temperature for 40 min in the dark to attain the adsorption–desorption equilibrium, then exposed to sunlight. The solution was then stirred by the magnetic stirrer in the presence of sunlight. At a particular time interval, dye solution was collected and centrifuged for 10 min to remove the Photocatalysts. The obtained solution was used to measure the progress of photocatalytic degradation of MO and MB by recording the absorbance using a UV–Vis spectrophotometer (Specord 200 plus, Analytikjena, Germany).

Results and Discussion

In order to confirm the crystalline structure of synthesized TiO_2 photocatalyst, powder XRD pattern was studied, which is shown in the Fig. 1. The XRD pattern for the prepared sample shows the diffraction peaks at 2θ values in degree 25.28, 36.94, 37.80, 38.57, 48.04, 53.89, 55.06, 62.68, 68.76, 70.30, and 75.02. They are corresponds to (101), (103), (004), (112), (200), (105), (211), (204), (116), (220) and (215) reflections of anatase phase of TiO_2 [24], with reference to JCPDS Card No. 21-1272 and no other phases (brookite, rutile) were observed and the lattice parameter values are $a = b = 3.785$ and $c = 9.513$. The surface morphology of

TiO_2 sample was studied by using TEM technique. Figure 2a, b displays the TEM image for the as-prepared sample, as one can see from the figure, the sample consist of spindle-like morphology. The diameter of spindle is in the range of approximately 50–70 nm. The HRTEM image shown in Fig. 2c further substantiates the anatase phase of TiO_2 with the lattice spacing of 0.35 nm assigned to the (101) plane, which is consistent with the XRD result.

FT-IR technique is used to measure the chemical bonds present in the products. The FT-IR spectrum of spindle-like TiO_2 nanostructures calcined at 400 °C for 3 h is shown in Fig. 3. The FTIR bands observed at 3409 and 1621 cm^{-1} are due to the O–H stretching mode of hydroxyl group. The peaks located at 493, 443 and 428 cm^{-1} is likely due to the vibration of the TiO_2, which confirms the prepared sample is TiO_2 nanostructures. The optical properties were determined by UV–Vis spectroscopy. Figure 4a displays the characteristic absorption spectrum of spindle-like TiO_2 nanostructures. The absorption edge value of spindle-like TiO_2

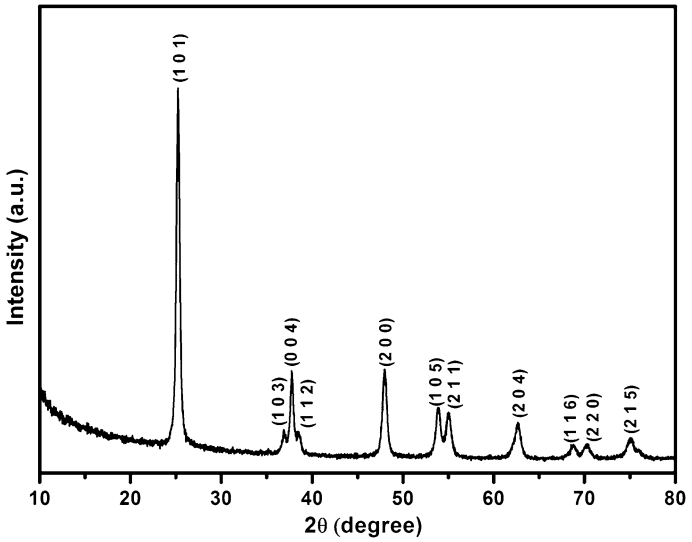

Fig. 1 XRD pattern of spindle-like TiO_2 nanostructure

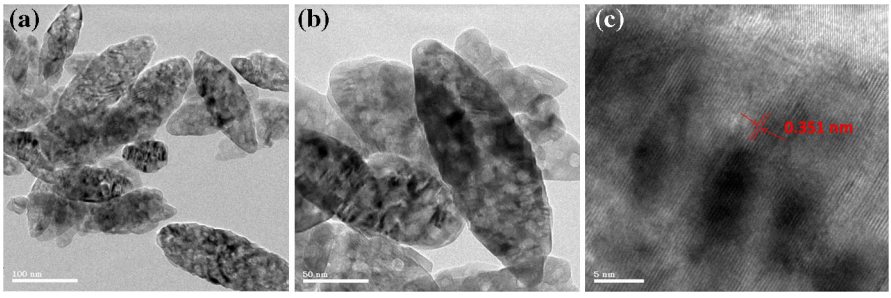

Fig. 2 **a** and **b** TEM image and **c** HRTEM image of spindle-like TiO_2 nanostructure

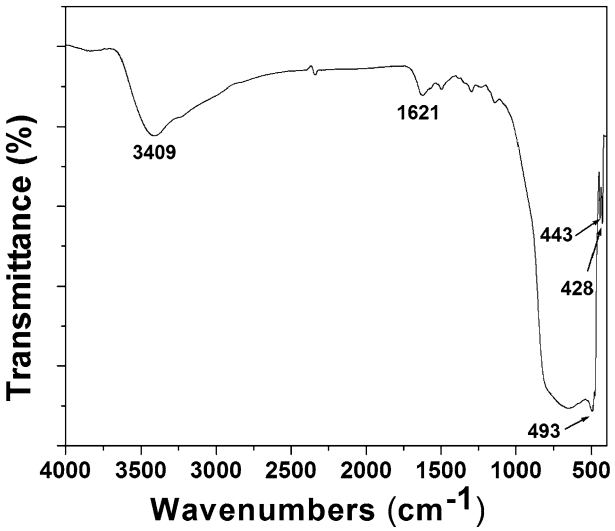

Fig. 3 FTIR spectrum of spindle-like TiO_2 nanostructure

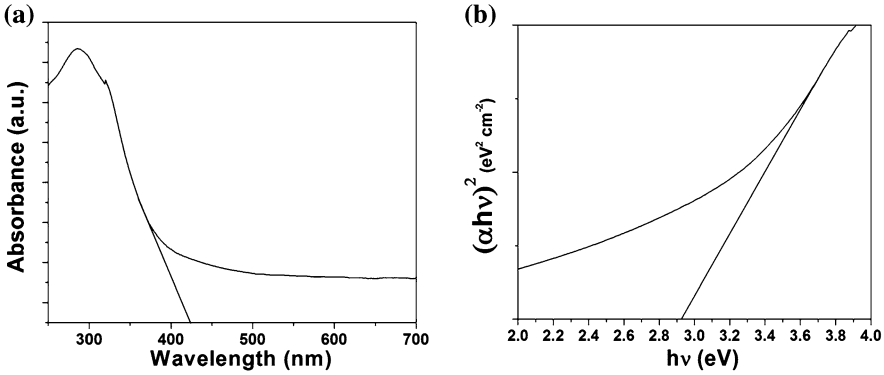

Fig. 4 **a** UV–Visible spectrum and **b** Band gap plot [hν vs $(\alpha h\nu)^2$] of spindle-like TiO_2 nanostructure

nanostructure is calculated to be 423 nm. The absorption coefficient for TiO_2 is determined by the following equation [25].

$$(\alpha h\nu)^{1/2} = h\nu - E_g$$

where hν is the photon energy, α is the optical absorption coefficient, E_g is the band gap energy, m = 1/2 or 3/2 represents the indirect allowed and indirect forbidden transitions, and m = 2 or 3 denotes the direct allowed and direct forbidden transitions. The band gap energy was measured by plotting $(\alpha h\nu)^2$ of TiO_2 against the photon energy (hν), as shown in Fig. 4b. Therefore, the band gap energy value of spindle-like TiO_2 nanostructures is 2.92 eV.

The photocatalytic degradation of MO and MB dye molecules under direct sunlight was used to measure the photocatalytic performance of spindle-like TiO_2 nanostructure, which is measured every 30 min during the photocatalysis experiments under sunlight irradiation. Figure 5a, b depicts the representative variations in the characteristic absorption of MO and MB under sunlight irradiation. The intensity of characteristic absorption peaks for MO and MB continuously reduces as the sunlight irradiation time increases, suggesting that MO and MB gradually degraded. Thus, the degradation of MO and MB was achieved after 150 min. Figure 6a, b shows the changes of the MO and MB relative concentrations (C/C_0) as a function of irradiation time t, where C is the concentration of MO or MB at the irradiation time t and C_0 is the initial concentration. It can be seen that the spindle-like TiO_2 nanostructure exhibited photocatalytic behaviors in the degradation of MO and MB. From earlier results on photodegradation activity of TiO_2, WO_3 and spindle-like WO_3-TiO_2 particles (diameter of 150 nm) were 38, 10 and 79% for the degradation of MO in 120 min [26], which is lower than what obtained in the present study (82.5% of MO degradation in 120 min). The result indicates that the prepared spindle-like TiO_2 nanostructure showed better photocatalytic degradation due to its smaller diameter (diameter of 50–70 nm) of spindle-like nanostructure. In another report, the pure spherical-like TiO_2 nanoparticles showed poor photocatalytic activity due to its limited photoresponding range and only 13% of the initial MB diminishes after more than 100 min [27], which is lower than the present results of 62.7% of MB degradation in 120 min. The present result showed that the synthesized TiO_2 sample showed better photocatalytic degradation owing to its spindle-like nanostructure. The main advantage of spindle-like TiO_2 nanostructure when compared with spherical particles, the spindle-like nanostructure has higher electron transfer capability of photo-injected electrons in the TiO_2 crystal lattice.

The stability and durability of the photocatalytic activity of the synthesized spindle-like TiO_2 nanostructures was measured by reuse of the catalysts under the sunlight irradiation. After the first cycle, the used photocatalyst was filtered and washed thoroughly with deionized water and reused in the subsequent reaction

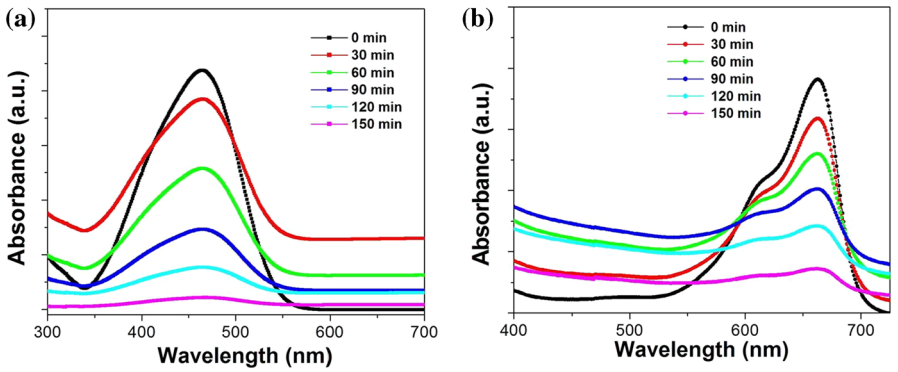

Fig. 5 UV–Vis absorption spectra of **a** MO and **b** MB solution in the presence of spindle-like TiO_2 photocatalyst under sunlight at 30 min intervals

(second, third, fourth and fifth cycle) under same conditions (150 min irradiation for each cycle). Figure 7 shows the recycled photocatalytic degradation of MO and MB, there is no significant change in the activity toward MB and MO after fifth successive recycles. The degradation rate is not decreasing on the whole after five cycles. The results indicated that the spindle-like TiO_2 nanostructure catalyst exhibited excellent photocatalytic activity, stability and durability. The recycles are in good agreement with those reported in the literature [28, 29]. The reaction mechanism of photocatalytic activity of the spindle-like TiO_2 nanostructure is shown in Fig. 8. Once the spindle-like TiO_2 nanostructure is irradiated with sun light, the electrons are excited from the valence band (VB) to the conduction band (CB), which lead to create holes in the VB and electron in the CB. The photoinduced hole reacts with adsorbed water molecules (or surface hydroxyl) thus producing hydroxyl radicals ($OH^{\cdot}$), which are responsible for the decomposition of the MO and MB dye into non-toxic products. Electron in the conduction band reacts with dissolved oxygen molecules to generate superoxide radical ion ($O_2^{\cdot -}$). Both radical groups ($OH^{\cdot}$ and $O_2^{\cdot -}$) are highly reactive toward MO and MB dye

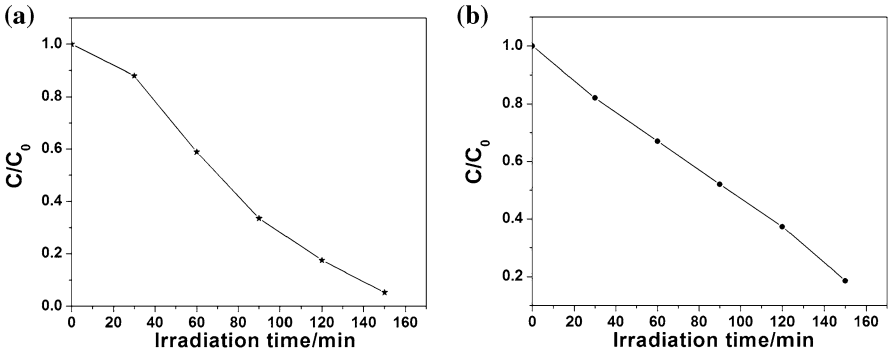

Fig. 6 C/C_0 curve for degradation of **a** MO and **b** MB under sunlight using spindle-like TiO_2 photocatalyst

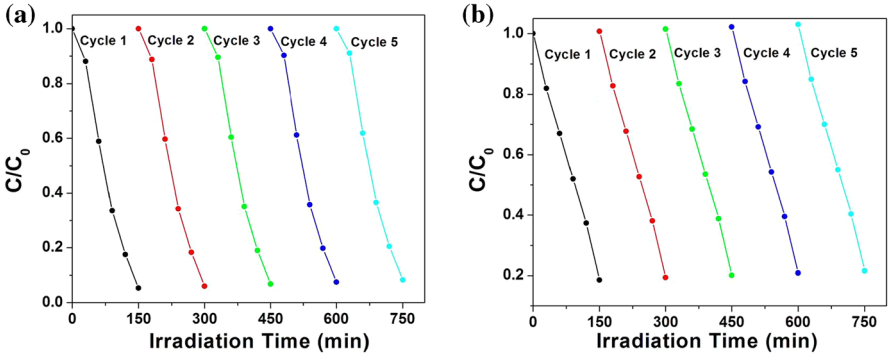

Fig. 7 Recycled photocatalytic degradation of **a** MO and **b** MB

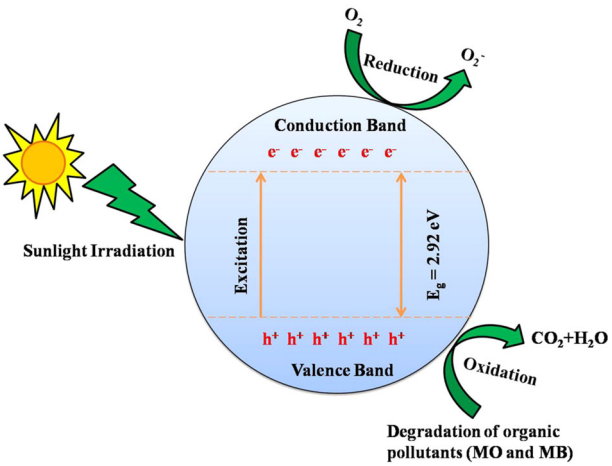

Fig. 8 The mechanism of photocatalytic activity of the spindle-like TiO_2 nanostructure

degradation under sun light illumination [28, 30]. The spindle-like TiO_2 could provide more active sites during the photocatalytic reaction, which is beneficial to photocatalytic degradation process.

Conclusion

Spindle-like TiO_2 nanostructures have been prepared through a solvothermal method followed by calcination at 400 °C for 3 h. The phase structure, morphology and optical properties of the synthesized sample were characterized by X-ray diffraction, transmission electron microscopy and ultraviolet spectroscopy. X-ray diffraction pattern showed that the prepared sample was TiO_2 with well-crystallized anatase phase. TEM images revealed that the TiO_2 sample composed of spindle-like shape with size in the range of 50–70 nm. Optical measurement showed that the band gap value of spindle-like TiO_2 nanostructures was 2.92 eV. The photocatalytic activity of the spindle-like TiO_2 nanostructures was measured by degradation of methyl orange and methyl blue and the spindle-like TiO_2 nanostructures exhibited excellent photocatalytic performance.

References

1. X. W. Wang, H. W. Tian, Y. Yang, H. Wang, S. M. Wang, W. T. Zheng, and Y. C. Liu (2012). *J. Alloys Compd.* **524**, 5.
2. A. A. Farghali, M. Bahgat, W. M. A. El Rouby, and M. H. Khedr (2013). *J. Alloys Compd.* **555**, 193.
3. H. Xua, C. T. Liu, H. M. Li, Y. G. Xu, J. X. Xia, S. Yin, L. Liu, and X. Y. Wu (2011). *J. Alloys Compd.* **509**, 9157.
4. L. Sun, R. Shao, L. Q. Tang, and Z. D. Chen (2013). *J. Alloys Compd.* **564**, 55.
5. L. Zhang, Y. M. He, P. Ye, Y. Wu, and T. H. Wu (2013). *J. Alloys Compd.* **549**, 105.

6. V. K. Garg, R. Gupta, A. B. Yadav, and R. Kumar (2003). *Bioresour. Technol.* **89**, 121.
7. S. M. Ghoreishi and R. Haghighi (2003). *Chem. Eng. J.* **95**, 163.
8. M. A. Kabil and S. E. Ghazy (1994). *Sep. Sci. Technol.* **29**, 2533.
9. D. W. Lee, W. H. Hong, and K. Y. Hwang (2000). *Sep. Sci. Technol.* **35**, 1951.
10. J. N. Wu, M. A. Eiteman, and S. E. Law (1998). *J. Environ. Eng.* **124**, 272.
11. X. P. Pu, D. F. Zhang, Y. Y. Gao, X. Shao, G. Q. Ding, S. S. Li, and S. P. Zhao (2013). *J. Alloys Compd.* **551**, 382.
12. T. Lv, L. K. Pan, X. J. Liu, T. Lu, G. Zhu, and Z. Sun (2011). *J. Alloys Compd.* **509**, 10086.
13. S. K. Li, F. Z. Huang, Y. Wang, Y. H. Shen, L. G. Qiu, A. J. Xie, and S. J. Xu (2011). *J. Mater. Chem.* **21**, 7459.
14. F. Z. Liu, X. Shao, J. Q. Wang, S. R. Yang, H. Y. Li, X. H. Meng, X. H. Liu, and M. Wang (2013). *J. Alloys Compd.* **551**, 327.
15. N. R. Khalid, Z. Hong, E. Ahmed, Y. Zhang, H. Chan, and M. Ahmad (2012). *Appl. Surf. Sci.* **258**, 5827.
16. C. Liu, X. Zhang, Q. Zhang, G. Meng, H. Zhao, J. Wu, and Z. Liu (2017). *J. Porous Mater.* **24**, 179.
17. A. S. Attar, M. S. Ghamsari, F. Hajiesmaeilbaigi, S. Mirdamadi, K. Katagiri, and K. Koumoto (2009). *Mater. Chem. Phys.* **113**, (2), 856.
18. X. J. Feng, J. Zhai, and L. Jiang (2005). *Angew. Chem. Int. Ed.* **44**, 5115.
19. Z. Ding, X. Hu, P. L. Yue, G. Q. Lu, and P. F. Greenfield (2001). *Catal. Today* **68**, 173.
20. P. Hoyer (1996). *Langmuir* **12**, 1411.
21. A. Hu, X. Zhang, K. D. Oakes, P. Peng, Y. N. Zhou, and M. R. Servos (2011). *J. Hazard. Mater.* **189**, 278.
22. L. Li, X. Qin, G. Wang, L. Qi, G. Du, and Z. Hu (2011). *Appl. Surf. Sci.* **257**, 8006.
23. J. Lee, Y. Lee, H. Song, D. Jang, and Y. Choa (2011). *Curr. Appl Phys.* **11**, S210.
24. J. Jiang, F. Gu, X. Ren, Y. Wang, W. Shao, C. Li, and G. Huang (2011). *Ind. Eng. Chem. Res.* **50**, 9003.
25. G. M. Kim, S. M. Lee, G. H. Michler, H. Roggendorf, U. Gosele, and M. Knez (2008). *Chem. Mater.* **20**, 3085.
26. D. Sun, J. Liu, J. Li, Z. Feng, L. He, B. Zhao, T. Wang, R. Li, S. Yin, and T. Sato (2014). *Mater. Res. Bull.* **53**, 163.
27. D. Zhao, G. Sheng, C. Chen, and X. Wang (2012). *Appl. Catal. B* **111–112**, 303.
28. L. Gnanasekaran, R. Hemamalini, and K. Ravichandran (2015). *J. Saudi Chem. Soc.* **19**, 589.
29. Y. Liu, H. Yu, Z. Lv, S. Zhan, J. Yang, X. Peng, Y. Ren, and X. Wu (2012). *J. Environ. Sci.* **24**, (10), 1867.
30. S. Thirumalairajan, K. Girija, V. R. Mastelaro, and N. Ponpandian (2014). *New J. Chem.* **38**, 5480.